

Harmonic Analysis of Inverter-Based Resources Subject to Unbalance

Rabi Kar, Zhixin Miao, Lingling Fan

Dept. of Electrical Engineering

University of South Florida

Tampa, USA

{rskar, zmiao, linglingfan}@usf.edu

Abstract—Operation of wind turbine generators is affected by unbalance in the grid voltage. This paper presents harmonic analysis when type-4 wind turbine is subjected to grid voltage unbalance. For simplicity, in the current research, the type-4 wind turbine’s grid-side converter is assumed to have constant dq -frame modulation indices. First, an EMT model for Type-4 wind turbine with unbalanced grid voltage is modeled in PSCAD. The current is found to have positive-, negative-sequence fundamental components as well as positive-sequence 180 Hz harmonic component. Steady-state circuit analysis is then carried out to compute the current harmonic components. The analysis results match the EMT simulation results.

Index Terms—Type-4 wind; EMT Model; steady-state analysis

I. INTRODUCTION

With the advancement of the modern power system and increased dependency on the electricity, the gradual shift of power generation is in course from nuclear, thermal generation to more renewable generation process. That being said one of the greatest innovation of modern power system are the wind turbines. The first of which was invented in 1888 in Cleveland, Ohio by Charles F. Brush. But the major advancement in wind turbines have occurred in the last decade.

Significantly large wind power generations are now widespread around the world. They are connected to the public network and to the grid. Grid connected operations of wind turbine generators (WTGs) can result in certain technical problems. One such issue is harmonics due to unbalance operation.

In [1] the author has explained different method of analysis of an unbalanced Wind Turbine. Most recently, [2] examined harmonics in grid-connected converter subject to unbalance and identified 3rd harmonics as the result of unbalance.

The current paper focuses on the effect of unbalanced grid voltage on a Type-4 wind model. Different from [2] where analysis is based on three-phase vectors, we adopt space vector based modeling for unbalance analysis. The space vector based analysis results in more concise expressions and clear insights.

The remainder of the paper is organized as follows. Section 2 presents the EMT model description and harmonic analysis when the converter is subject to grid voltage unbalance. Sec-

tion 3 presents the harmonic analysis. Voltage/current relationships of the DC side, the ac side, and the relationship between the DC and the AC side of the converter are thoroughly examined and mathematic relationship is formed. Section 4 concludes the paper.

II. EMT TESTBED RESULTS

Fig. 1 represents a equivalent circuit of a Type-4 wind farm. In this model, the synchronous generator and the rectifier circuit is designed as a constant voltage source in series with an inductor, L_{dc} of 1 mH and a DC link capacitor, C_{dc} of 7500 μ F to ignore the machine dynamics. The voltage source converter (VSC) is designed as a detailed model with six IGBT switches with a switching frequency of 1 kHz. The grid is connected to the PCC bus through a RL transmission line with X_{line} as 0.1 pu and $\frac{R_{line}}{X_{line}} = 0.1$. The parameters in SI unit is stated in Table I.

The converter ac side is connected with a low-pass filter to minimize the effect of harmonics on the grid. In the Fig. 1, R and L represent total Resistance and Induction of the system from the converter to the grid. The EMT model in Fig. 1 is modeled in PSCAD V4.6. The model is built based on the reference provided in [3].

TABLE I: Parameters

Parameters	Values (SI)
V_{grid}	391.9 V
R_{line}	0.0219 Ω
X_{line}	582 μ H
L_{filter}	125 μ H
C_{filter}	200 μ F
L_{damp}	625 μ H
C_{damp}	100 μ F
R_{damp}	2.5 Ω

1) *Low Pass Filter*: To eliminate the enormous amount of harmonics generated by the inverter, a good design of a low-pass filter is necessary. The detail design of the low-pass LCL filter in Fig. 1, is expanded in Fig. 2. The detailed parameter selection procedure of the low pass filter is described in PSCAD handbook, [3], and the final value of the parameters is shown in Table I.

A. Simulation result

The Type-4 wind detailed model from PSCAD example is considered to be the benchmark model. To create an unbalance

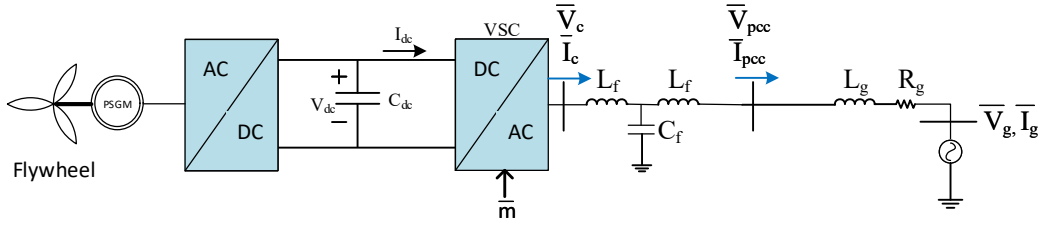


Fig. 1: Equivalent model for type-4 wind farm.

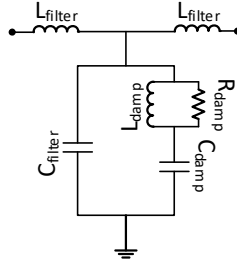


Fig. 2: LCL filter.

in the grid voltage, a voltage sag of 0.3 pu has been introduced at 0.3 secs as shown in Fig. 3. In real world, a voltage dip may appear due to an unbalanced load in the grid side or a single line to ground fault on phase-a long transmission line. The unbalance in the grid voltage will result in two components of the grid voltage, 60 Hz component in positive sequence and 60 Hz component in negative sequence. The phasor form of the three-phase grid voltage v_{grid} is expressed as the follows. Note that the real parts are the three-phase signals.

$$\bar{v}_{\text{grid}} = \begin{bmatrix} \hat{V}'_g e^{j0} \\ \hat{V}'_g e^{j(-\frac{2\pi}{3})} \\ \hat{V}'_g e^{j(+\frac{2\pi}{3})} \end{bmatrix} = \begin{bmatrix} 0.7 \\ e^{j(-\frac{2\pi}{3})} \\ e^{j(+\frac{2\pi}{3})} \end{bmatrix} \times 0.4 \text{ kV} \quad (1)$$

where \hat{V}'_g represents the unbalanced voltage magnitude in phase-a.

From Eq. (1), we can derive the positive and negative sequence as below,

$$\begin{bmatrix} \bar{V}_{\text{grid}}^{(+)} \\ \bar{V}_{\text{grid}}^{(-)} \end{bmatrix} = \frac{1}{3} \begin{bmatrix} 1 & \alpha & \alpha^2 \\ 1 & \alpha^2 & \alpha \end{bmatrix} \begin{bmatrix} \hat{V}'_g e^{j0} \\ \hat{V}'_g e^{j(-\frac{2\pi}{3})} \\ \hat{V}'_g e^{j(+\frac{2\pi}{3})} \end{bmatrix} = \begin{bmatrix} 0.36 \\ -0.04 \end{bmatrix} \text{ kV} \quad (2)$$

where $\alpha = e^{j\frac{2\pi}{3}}$.

Unbalanced condition Eq. (2) will provide a negative-sequence component. FFT analysis of the sequential diagram shown in Fig. 4 verifies the above analysis. The frequency step in the FFT plot is 10 Hz.

In the space vector form we can represent the unbalanced grid voltage as the sum of positive and negative sequence

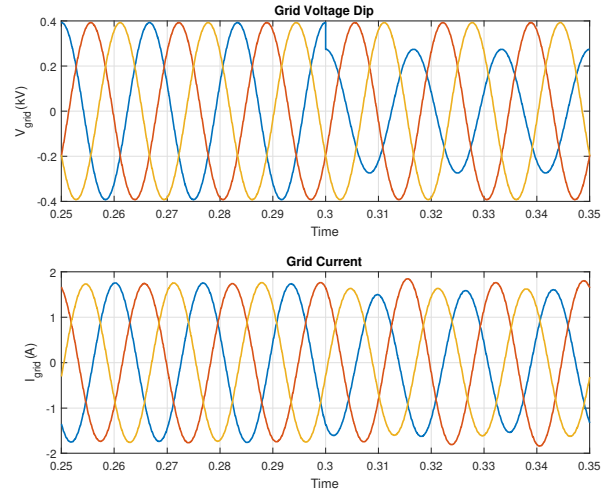


Fig. 3: Voltage dip.

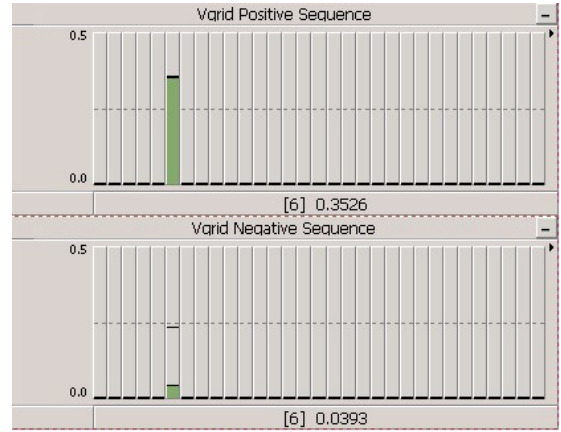


Fig. 4: FFT plot showing positive and negative voltages for grid voltage. Positive sequence component: 0.35 kV, negative sequence component: 0.04 kV.

voltage as shown in Eq. (3),

$$\vec{v}_{\text{grid}} = \bar{V}_{\text{grid}}^{(+)} e^{j\omega_0 t} + \bar{V}_{\text{grid}}^{(-)*} e^{-j\omega_0 t} \quad (3)$$

where the superscript * notates complex conjugate.

EMT simulation results show that the converter voltage and current will have fundamental component and a 3rd harmonic component in the positive sequence and a fundamental com-

ponent in the negative sequence. The sequence diagram from the EMT testbed is shown in Figs. 5 and 6.

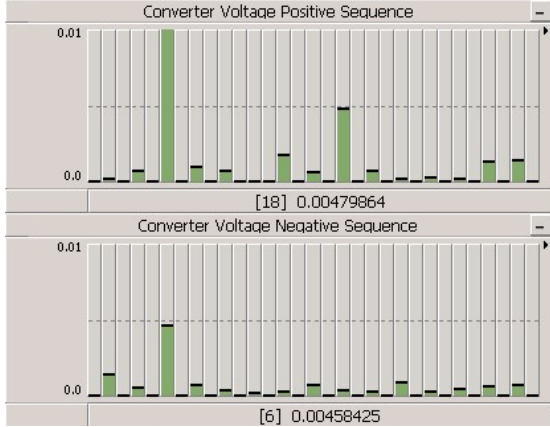


Fig. 5: FFT plot showing positive and negative voltages for converter voltage.

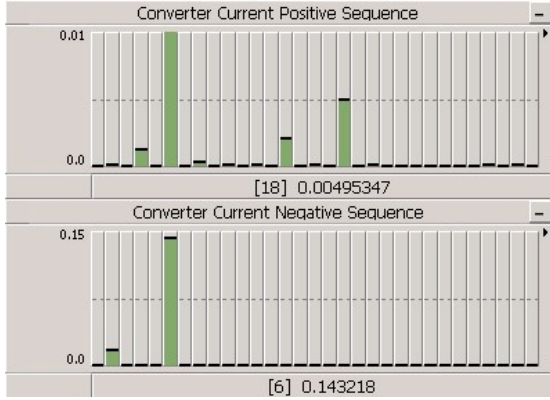


Fig. 6: FFT plot showing positive and negative sequence currents for converter current.

The components will be computed using the steady-state analysis in Section 3.

Due to the unbalanced voltage dip occurring in the grid side, the AC power will also have a second harmonic component along with the DC component. Since the power loss in case of inverter is zero, the DC power also has a second harmonic component. So the DC-link voltage and current will also have a second harmonic component. Fig. 7 shows the oscillation of the DC-link voltage and current. The presence of second harmonic component on the DC-link voltage and current can also be verified from the FFT analysis of the DC side voltage and current as shown in Fig. 8.

III. STEADY-STATE ANALYSIS

In this section we conduct steady-state analysis. The emphasize is the grid-connected converter's dc side and ac side. The combination of synchronous generator and the AC to DC rectifier model shown in Fig. 1 is replaced by an ideal DC voltage source in series with an Inductor of 1 mH and a DC-link capacitor of 7500 μ F as shown in Fig. 10. The DC-link voltage is the voltage measured across the DC-link capacitor

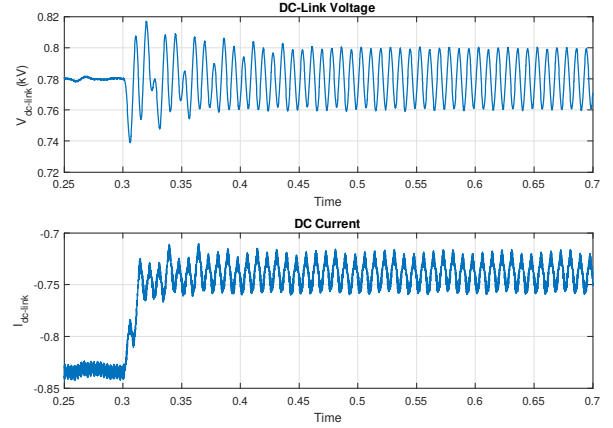


Fig. 7: DC-Link voltage and current.

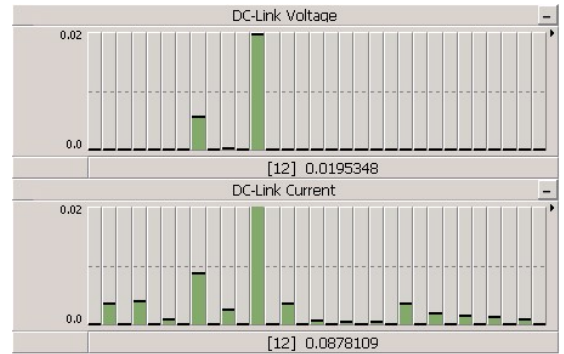


Fig. 8: FFT Magnitude Plot for DC-Link voltage and current.

and the DC current is the current flowing into the inverter circuit.

A. AC side voltage/current relationship

In this section we are going to analyze the connection between the converter and the grid represented inside the rectangular box shown in Fig. 9. For simplicity of derivation the total impedance between the converter and the grid bus is represented as R_{total} and L_{total} .

$$R_{total} = R_{filter} + R_{line} \quad \text{and}$$

$$L_{total} = L_{filter} + L_{line}$$

In the system shown in Fig. 9, we assume power flow is from the converter to the grid. So the KVL equation from the converter to the grid is represented in Eq. (4).

$$\vec{v}_{conv} - \vec{v}_{grid} = (R_{total} + sL_{total}) \times \vec{i}_{conv} \quad (4)$$

Dq-frame Analysis: Eq. (4) can be represented in the dq -frame:

$$\bar{V}_{conv} - \bar{V}_{grid} = (R_{total} + (s + j\omega_0)L_{total})\bar{I}_{conv} \quad (5)$$

We assume in the dq -frame,

$$\bar{V} = v_d + jv_q$$

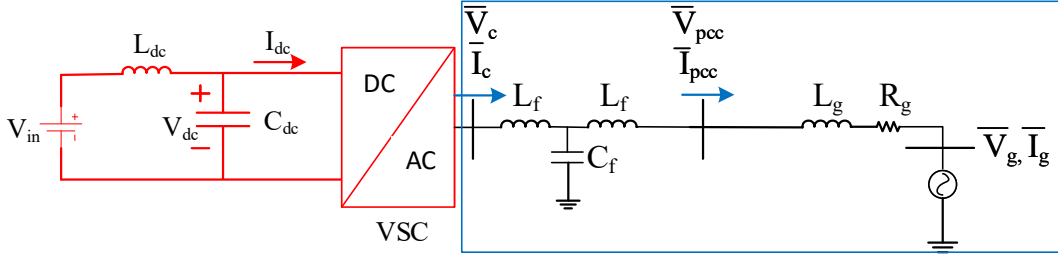


Fig. 9: Equivalent circuit of Type-4 converter: emphasis on the grid side.

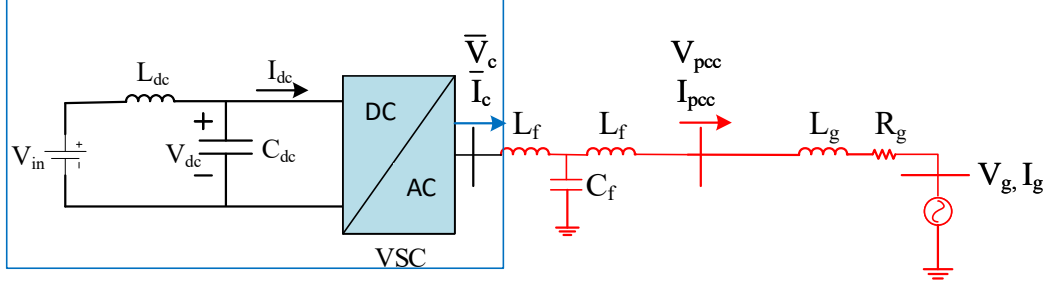


Fig. 10: Equivalent circuit of Type-4 converter: emphasis on the DC side.

So Eq. (5) can be expressed as the following.

$$\begin{bmatrix} v_{\text{conv},d} \\ v_{\text{conv},q} \end{bmatrix} - \begin{bmatrix} v_{\text{grid},d} \\ v_{\text{grid},q} \end{bmatrix} = \begin{bmatrix} R_{\text{total}} + sL_{\text{total}} & -\omega_0 L_{\text{total}} \\ \omega_0 L_{\text{total}} & R_{\text{total}} + sL_{\text{total}} \end{bmatrix} \begin{bmatrix} i_{\text{conv},d} \\ i_{\text{conv},q} \end{bmatrix} \quad (6)$$

Under unbalanced condition, the system will show the presence of both 0 Hz component and 120 Hz component in the dq-frame. Under unbalanced condition, relationship among the 120 Hz components can be represented by Eq. (7). The 120 Hz component is represented by a superscript (2), (*)(2).

$$\begin{bmatrix} \overline{v}_{\text{conv},d}^{(2)} \\ \overline{v}_{\text{conv},q}^{(2)} \end{bmatrix} - \begin{bmatrix} \overline{v}_{\text{grid},d}^{(2)} \\ \overline{v}_{\text{grid},q}^{(2)} \end{bmatrix} = \begin{bmatrix} R_{\text{total}} + L_{\text{total}}s^{(2)} & -\omega_0 L_{\text{total}} \\ \omega_0 L_{\text{total}} & R_{\text{total}} + L_{\text{total}}s^{(2)} \end{bmatrix} \begin{bmatrix} \overline{i}_{\text{conv},d}^{(2)} \\ \overline{i}_{\text{conv},q}^{(2)} \end{bmatrix} \quad (7)$$

where $s^{(2)} = j2\omega_0$.

Phasor-domain analysis

To analyze the unbalanced condition in phasor-domain, the voltage and current are decomposed to positive and negative sequence components. It is known that the system has three harmonic components: positive-sequence fundamental component, negative sequence fundamental component, and positive sequence 3rd harmonic component.

Equation Eq. (4) under unbalanced condition can be decomposed in three different equations representing fundamental component in positive sequence, 3rd harmonic component in positive sequence and fundamental sequence in negative

sequence as represented in Eqs. (8) to (10). The superscript (+), (3) and (-) represent fundamental component in positive sequence, 3rd harmonic in positive sequence and fundamental component in negative sequence respectively.

$$\overline{V}_{\text{conv}}^{(+)} - \overline{V}_{\text{grid}}^{(+)} = (R_{\text{total}} + L_{\text{total}}s^{(+)}) \times \overline{I}_{\text{conv}}^{(+)} \quad (8)$$

$$\overline{V}_{\text{conv}}^{(3)} - \overline{V}_{\text{grid}}^{(3)} = (R_{\text{total}} + L_{\text{total}}s^{(3)}) \times \overline{I}_{\text{conv}}^{(3)} \quad (9)$$

$$\overline{V}_{\text{conv}}^{(-)} - \overline{V}_{\text{grid}}^{(-)} = (R_{\text{total}} + L_{\text{total}}s^{(-)}) \times \overline{I}_{\text{conv}}^{(-)} \quad (10)$$

With a fundamental frequency represented as $\omega_0 = 377$ rad/sec, the Laplacian operator s can be represented as $s^{(+)} = j\omega_0$, $s^{(3)} = j3\omega_0$ and $s^{(-)} = -j\omega_0$.

To analyze unbalanced condition for converter to grid inter-connection we just consider Eqs. (9) and (10).

B. DC side and DC/AC relationship

In this section we are going to analyze the relation between the DC side and AC side voltage and current under unbalanced condition. The rectangular box in Fig. 10 is the part discussed in this section.

From Fig. 10, the relationship between the DC-Link voltage and the DC current is represented as,

$$V_{dc} = -Z_{dc}i_{dc} \quad (11)$$

where

$$Z_{dc} = L_{dc}s \parallel \frac{1}{C_{dc}s} \quad (12)$$

Under unbalanced condition the DC voltage and current will have second harmonic components, so the Laplacian operator,

s we be represented as $s^{(2)} = j2\omega_0$ and Eq. (12) will be represented as follows.

$$Z_{dc}^{(2)} = L_{dc}s^{(2)} \parallel \frac{1}{C_{dc}s^{(2)}} \quad (13)$$

Let's analyze the the DC and AC side of a converter using the power equivalent equation. The power conservation law is described as follows.

$$V_{dc}i_{dc} = \frac{3}{2} \text{Real}\{\bar{V}_{\text{conv}}\bar{I}_{\text{conv}}\} \quad (14)$$

DC side instantaneous power is equal to the ac side instantaneous power. The relationship between dc voltage V_{dc} and the ac converter \bar{V}_{conv} is as follows

$$\bar{V}_{\text{conv}} = \frac{\bar{m}}{2}V_{dc} \quad (15)$$

where $\bar{m} = m_d + jm_q$ is the phasor of the modulation indices. m_d and m_q in this paper are assumed to be constant for simplicity.

Substituting value of \bar{V}_{conv} in Eq. (14) leads to

$$\begin{aligned} i_{dc} &= \frac{3}{4} [m_d \quad m_q] \begin{bmatrix} i_{\text{conv},d} \\ i_{\text{conv},q} \end{bmatrix} = \text{Real}\{\bar{m}\bar{I}_{\text{conv}}^*\} \\ &= \frac{3}{8} (\bar{m}\bar{I}_{\text{conv}}^* + \bar{m}^*\bar{I}_{\text{conv}}) \\ &= \frac{3}{8} (\bar{m}\vec{i}_{\text{conv}}^* e^{j\omega_0 t} + \bar{m}^*\vec{i}_{\text{conv}} e^{-j\omega_0 t}) \end{aligned} \quad (16)$$

Under unbalanced condition, for the 120 Hz harmonic component in the dq -frame and dc side, Eqs. (11), (15) and (16) can be represented as follows.

$$\bar{V}_{dc}^{(2)} = -Z_{dc}^{(2)}\bar{I}_{dc}^{(2)} \quad (17)$$

$$\begin{bmatrix} \bar{V}_{\text{conv},d}^{(2)} \\ \bar{V}_{\text{conv},q}^{(2)} \end{bmatrix} = \begin{bmatrix} m_d \\ m_q \end{bmatrix} \times \frac{\bar{V}_{dc}^{(2)}}{2} \quad (18)$$

$$\bar{I}_{dc}^{(2)} = \frac{3}{4} [m_d \quad m_q] \begin{bmatrix} \bar{I}_{\text{conv},d}^{(2)} \\ \bar{I}_{\text{conv},q}^{(2)} \end{bmatrix} \quad (19)$$

where the superscript (2) represents second harmonic component.

Phasor-domain analysis According to Fig. 10, the relationship between the DC link voltage and current will be same for both DQ and phasor domain analysis and can be expressed as,

$$V_{dc} = -Z_{dc}i_{dc} \quad (20)$$

Now to derive the relationship between converter voltage and DC link voltage, Eq. (15) can be used. Under unbalanced condition, DC-link voltage has 2 components, DC-component and 120 Hz component in positive and negative sequence. So the expression for DC-link voltage can be written as,

$$v_{dc} = V_{dc}^{(0)} + \frac{\bar{V}_{dc}^{(2)} e^{j2\omega_0 t} + \bar{V}_{dc}^{(2)*} e^{-j2\omega_0 t}}{2} \quad (21)$$

The relationship between converter voltage space vector and the DC-link voltage can be expressed as:

$$\vec{v}_{\text{conv}} = \frac{\bar{m}}{2} e^{j\omega_0 t} v_{dc} \quad (22)$$

Now from Eqs. (21) and (22), the expression of converter voltage can be written as,

$$\begin{aligned} \vec{v}_{\text{conv}} &= \frac{\bar{m}}{2} e^{j\omega_0 t} V_{dc}^{(0)} + \frac{\bar{m}}{4} e^{-j\omega_0 t} \bar{V}_{dc}^{*(2)} \\ &\quad + \frac{\bar{m}}{4} e^{j3\omega_0 t} \bar{V}_{dc}^{(2)} \end{aligned} \quad (23)$$

From Eq. (23) it is clear that under unbalanced condition, the converter voltage can be expressed in positive and negative sequence component and has a frequency component of 60 Hz and 180 Hz in positive sequence and another 60 Hz component in negative sequence.

The expression for 3rd Harmonic and negative 60 Hz component of the system can be expressed as:

$$\bar{V}_{\text{conv}}^{(-)} = \frac{\bar{m}^*}{4} \bar{V}_{dc}^{(2)} \quad (24a)$$

$$\bar{V}_{\text{conv}}^{(3)} = \frac{\bar{m}}{4} \bar{V}_{dc}^{(2)} \quad (24b)$$

Since Eq. (23) confirms that the converter side has a fundamental and 3rd harmonic component in positive sequence and a fundamental component in negative sequence, the converter side current can be expressed as the follows.

$$\vec{i}_{\text{conv}} = \bar{I}^{(+)} e^{j\omega_0 t} + \bar{I}^{*(-)} e^{-j\omega_0 t} + \bar{I}^{(3)} e^{j3\omega_0 t} \quad (25)$$

The phasor representation of the dc side current and converter current can be expressed from Eq. (16) as follows:

$$i_{dc} = \frac{3}{8} (\bar{m}\vec{i}_{\text{conv}}^* e^{j\omega_0 t} + \bar{m}^*\vec{i}_{\text{conv}} e^{-j\omega_0 t}). \quad (26)$$

By substituting Eq. (25) into Eq. (26), we can derive the final relationship between dc side current and converter side current under unbalanced conditions. The final equation can be split into two equations, shown on the following.

$$I_{dc}^{(0)} = \frac{3}{8} (\bar{m}\bar{I}_{\text{conv}}^{*(+)} + \bar{m}^*\bar{I}_{\text{conv}}^{(+)}) \quad (27a)$$

$$\bar{I}_{dc}^{(2)} = \frac{3}{4} (\bar{m}\bar{I}_{\text{conv}}^{(-)} + \bar{m}^*\bar{I}_{\text{conv}}^{(3)}) \quad (27b)$$

It can be seen that the dc-link current's 0 Hz component is related to the positive-sequence fundamental component of the ac side current, while the dc side current's 120 Hz component is related to the negative sequence fundamental component and 3rd harmonic component in the ac current.

The expressions in Eqs. (9), (10), (17), (24a), (24b) and (27b) can be used to analyze the system and find the value of $\bar{V}_{dc}^{(2)}$, $\bar{I}_{dc}^{(2)}$, $\bar{V}_{\text{conv}}^{(-)}$, $\bar{V}_{\text{conv}}^{(3)}$, $\bar{I}_{\text{conv}}^{(-)}$ and $\bar{I}_{\text{conv}}^{(3)}$. Algorithm 1 describes the computing procedure.

C. Validation

The simulation output from the EMT testbed shown in Fig. 8 can be validated using the equations in Section III-B. Using Algorithm 1 the numerical calculation was completed using MATLAB v2017b and the comparison is shown in Tables II and III.

It can be seen that the analysis results match well with the EMT simulation results.

Algorithm 1: Phasor domain analysis

Initialize the R, L and C;

$$s = j\omega_0;$$

$$s^{(2)} = 2\omega_0;$$

$$s^{(3)} = j3\omega_0;$$

$$s^{(-)} = -j\omega_0;$$

Initialize the modulation index;

Initialize v_{grid} ;

Process: Convert v_{grid} to sequence domain;

Define Variable: $\bar{V}_{\text{conv}}^{(-)}, \bar{V}_{\text{conv}}^{(3)}, \bar{I}_{\text{conv}}^{(-)}, \bar{I}_{\text{conv}}^{(3)}, \bar{V}_{\text{dc}}^{(2)}, \bar{I}_{\text{dc}}^{(2)}$;

Solve: Eqs. (9), (10), (17), (24a), (24b) and (27b).

TABLE II: Comparison between EMT Testbed and circuit analysis for different modulation index

		EMT Testbed	Analysis
$\bar{m} = 1 \angle 1.57$	$\bar{V}_{\text{conv}}^{(3)}$	0.0062 \angle 2.9776	0.0056 \angle 3.04
	$\bar{V}_{\text{conv}}^{(-)}$	0.0061 \angle -0.155	0.0056 \angle -0.09
	$\bar{I}_{\text{conv}}^{(3)}$	0.0049 \angle -1.42	0.0054 \angle -1.63
	$\bar{I}_{\text{conv}}^{(-)}$	0.143 \angle -1.677	0.1092 \angle -1.66
$\bar{m} = 0.8 \angle 1.57$	$\bar{V}_{\text{conv}}^{(3)}$	0.0037 \angle 3.02	0.0035 \angle 3.05
	$\bar{V}_{\text{conv}}^{(-)}$	0.0037 \angle -0.25	0.0035 \angle -0.13
	$\bar{I}_{\text{conv}}^{(3)}$	0.0029 \angle -1.42	0.0036 \angle -1.63
	$\bar{I}_{\text{conv}}^{(-)}$	0.135 \angle -1.673	0.1349 \angle -1.66

TABLE III: Comparison between EMT Testbed and circuit analysis for DC-Link side with different modulation index

		EMT Testbed	Analysis
$\bar{m} = 1 \angle 1.57$	$\bar{V}_{\text{dc}}^{(2)}$	0.0243 \angle -1.46	0.0227 \angle -1.663
	$\bar{I}_{\text{dc}}^{(2)}$	0.1113 \angle 3.043	0.1017 \angle 3.045
$\bar{m} = 0.8 \angle 1.57$	$\bar{V}_{\text{dc}}^{(2)}$	0.018 \angle -1.4664	0.0173 \angle -1.66
	$\bar{I}_{\text{dc}}^{(2)}$	0.083 \angle 3.0366	0.0787 \angle 3.05

IV. CONCLUSION

This paper has presented a steady-state problem formulation to find harmonic components of current and voltage when a type-4 wind is subject to unbalance. The analysis approach adopted is space-vector based modeling of three-phase signals as well as circuit analysis. The computing results show a close match of the EMT testbed for the steady state analysis algorithm.

REFERENCES

- [1] E. Muljadi, C. Butterfield, T. Batan, and D. Yildirim, "Understanding the Unbalanced-Voltage Problem in Wind Turbine Generation," Tech. Rep., 1999. [Online]. Available: <http://www.doe.gov/bridgehttp://www.nrel.gov/wind>
- [2] S. F. Zarei, H. Mokhtari, M. A. Ghasemi, S. Peyghami, P. Davari, and F. Blaabjerg, "Control of grid-following inverters under unbalanced grid conditions," *IEEE Transactions on Energy Conversion*, vol. 35, no. 1, pp. 184–192, 2020.
- [3] "Knowledge Base — PSCAD." [Online]. Available: <https://www.pscad.com/knowledge-base/article/227>